

HORIZONTAL TURBULENT DIFFUSION AT SEA SURFACE FOR OIL TRANSPORT SIMULATION

Yoshitaka Matsuzaki¹, Isamu Fujita²

In numerical simulations of oil transport at the sea surface, it is not known how to determine the horizontal turbulent diffusion coefficient of the oil. In this study, a model of diffusion at the sea surface was constructed to predict the turbulent diffusion coefficient of oil, based on results from drift experiments in a real sea using pseudo oil made of sponge rubber. Under experimental conditions, it was found that the diffusion coefficient at the sea surface was larger than under water, and that it does not depend on wind velocity or current velocity. We conducted numerical simulations using the derived diffusion model, which provided better results than traditional methods in the initial stages of an oil spill. The derived diffusion model is simple and therefore, easily incorporated into diffusion models of other oil transport simulations.

Keywords: oil spill; numerical simulation; real sea; drift experiments; horizontal turbulent diffusion

INTRODUCTION

In many numerical simulations of oil transport at the sea surface, based on a Lagrangian oil particle model, the oil turbulent diffusion is calculated using the random walk technique. The horizontal turbulent diffusion velocity U_{di} of a certain oil particle i is calculated by equation (1).

$$U_{di} = \sqrt{\frac{2D_H}{\Delta t}} \begin{bmatrix} R_{n1} \\ R_{n2} \end{bmatrix} \quad (1)$$

where D_H is the horizontal turbulent diffusion coefficient, Δt is the time step, and R_{n1} , R_{n2} are normal random numbers of averages are 0 and variances are 1. The random walk method needs a horizontal turbulent diffusion coefficient, as in equation (1), where a constant number is used for D_H . However, the horizontal turbulent diffusion velocity U_{di} is proportional to the one-half power of D_H ; therefore, the area of oil spread is proportional to D_H and thus, the numerical simulation results is affected by D_H .

The results of numerical simulations of oil turbulent diffusion vary considerably depending on the value of D_H used in the random walk technique, but this value is derived empirically. For example, the value of D_H is typically within the range of 1 - 100 m²/s (ASCE, 1996), which means that the simulated oil diffusion area has a range of the order of 10².

Many turbulent diffusion measurement experiments have been conducted using dyes or drifting buoys in the real sea. For example, Okubo (1971) conducted turbulent diffusion experiments using dye to explain the relationship between diffusion scale and the horizontal turbulent diffusion coefficient. Yanagi et al. (1982) conducted experiments using 50 60-cm-wide wooden floats each with a resistance board 1 m below the water surface. Michida et al. (2009) conducted experiments using GPS-tracked surface drifters with a drogue 1, 6, 11, and 16 m below the water surface. Their experimental results measured and estimated D_H under the water surface. However, the observation and estimation of D_H at the sea surface for oil have not been considered.

In this study, we conducted horizontal turbulent diffusion measurement experiments at the sea surface using pseudo oil to derive an expression for the calculation of D_H . We incorporated the diffusion model in our numerical simulation model to predict oil transport at the sea surface, and conducted hindcast simulations of an oil spill incident in Korea to verify the validity of the derived expression.

SELECTION OF PSEUDO OIL FOR DRIFT EXPERIMENTS IN A WIND CHANNEL TANK

To measure horizontal turbulent diffusion at the sea surface to simulate oil diffusion, the pseudo oil used in the real sea experiments has to move at the water surface only, and its drift characteristics must be the same as a real oil slick. The current-driven velocities of a real oil slick and the pseudo oil are the same; therefore, the pseudo oil should be selected to have the same wind coefficient.

In the numerical simulations, the wind-driven speed of movement of oil was estimated as 3% of the wind velocity at 10 m above the sea surface, i.e., "3%" represents the wind coefficient. For example, when

¹Marine Information and Tsunami Division, Port and Airport Research Institute, Japan, matsuzaki-y@pari.go.jp

²Frontier Technology and Engineering Division, Port and Airport Research Institute, Japan

Table 1: Relationship between wind velocity at 10 m above the water surface and wind coefficient

Blower rotation frequency (rpm)	Wind velocity at 10 m above the water surface (m/s)	Sponge rubber sheet movement velocity (m/s)	Wind coefficient	Standard deviation of wind coefficient
100	3.8	0.12	0.032	0.0011
200	6.3	0.18	0.030	0.0022
300	9.4	0.25	0.026	0.0021

wind velocity at 10 m above the sea surface is 10 m/s, the velocity of movement of an oil slick on the surface of the water surface can be calculated as $10 \times 0.03 = 0.30$ m/s. Therefore, the pseudo oil used in the real sea experiments had to have the same wind coefficient.

Experiments to select the most appropriate pseudo oil were conducted in a wind channel tank. The wind channel tank used was 28.5-m long, 1.5-m wide, 1.3-m high, with a depth of 0.4 m. The pseudo oil was made from sponge rubber sheet (INOAC EPDM Type, Part number E-4388, Hardness 20 ± 5 , Density 150 kg/m^3). The sponge rubber sheet used in the real sea experiments had a diameter of 1 m; however, that size could not be accommodated in the wind channel tank. Thus, the size of the model sponge rubber sheet used in the tank experiments was 30 cm in diameter and 10-mm thick. Furthermore, a GPS logger was attached to each pseudo oil sheet in the real sea experiments and thus, the weight of the GPS logger was added to the model sponge rubber sheet.

The experiments in the wind channel tank were conducted as follows. Wind velocity was set in a triple pattern (Blower rotation frequency: 100, 200, and 300 rpm). The model sponge rubber sheet, placed at the upwind end of the tank, had sufficient acceleration length when the wind-driven current attained steady flow. Photographs of the moving model sponge rubber sheet were taken at a position 19.5 m from the wind inlet and the velocity of movement calculated based on the center positions of the model sponge rubber sheet.

Wind velocities were measured at 18.0 and 21.0 m from the wind inlet using a thermal anemometer (Model number; 0962-00, KANOMAX JAPAN INC., Japan). The wind velocity at 10 m above the sea surface is commonly used for the oil transport simulations; thus, the tank experiments considered the same wind conditions. The wind velocity at 10 m above the water surface was calculated using the following method. Two measurement points were used for the analysis. The wind was observed for 60 seconds and the values averaged for every 5-mm elevation from the non-contact height of the wind-induced waves to about 10 cm from the calm water surface. It was assumed that the vertical profile of the averaged wind velocity followed a logarithmic law, and the distribution of wind velocity was estimated using the least squares method from which the wind velocity at 10 m above the water surface was interpolated.

The experimental results are shown in Table 1. The maximum average wind velocity during the experiment in the real sea was about 7 m/s; thus, the experimental conditions in the wind channel tank included the real sea experimental conditions. The wind coefficients were approximately 0.03; therefore, the sponge rubber sheet was deemed suitable for simulating oil diffusion on the sea surface.

EXPERIMENTAL METHOD OF DRIFT EXPERIMENTS IN THE REAL SEA

The real sea experiments were conducted at the mouth of Tokyo Bay in Yokosuka, Japan (Fig. 1). Figure 2 illustrates the experimental method. The drifting oil was represented by 20 objects (pseudo oil) made of the same sponge rubber sheet as used in the tank experiments, each 1 m in diameter and 10-mm thick (Fig. 3). A small GPS logger (Model number; WBT-202, dimensions: $64 \times 40 \times 17$ mm, weight; 55 g, accuracy CEP (Circular Error Probability); 2.0 m (SBAS)/2.5 m (stand-alone), Wintec Co. Ltd, Taiwan) was attached to each pseudo oil object. In each experimental case, the 20 pseudo oil objects were followed by an observation ship, which recorded wind velocity and direction using an anemometer (Model number; WindSonic PGWS-100, Gill Instruments Limited., UK) positioned 4 m above the sea surface, and the GPS loggers recorded the position of each pseudo oil objects. The wind data were measured every second and averaged over 10-minute intervals. Current velocity and direction were measured using an acoustic Doppler current profiler (Model number; Sentinel ADCP 1200 kHz, Teledyne RD Instruments, USA). The current velocity could be measured at 1.5 m below the sea surface. The measurement time interval was about 20

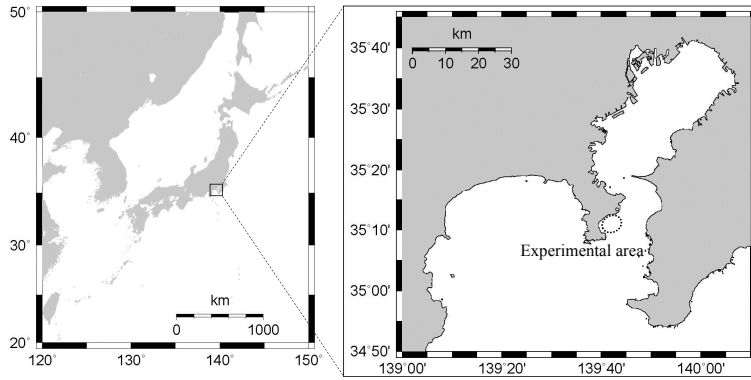


Figure 1: The real sea experiments were conducted at the mouth of Tokyo Bay in Yokosuka, Japan.

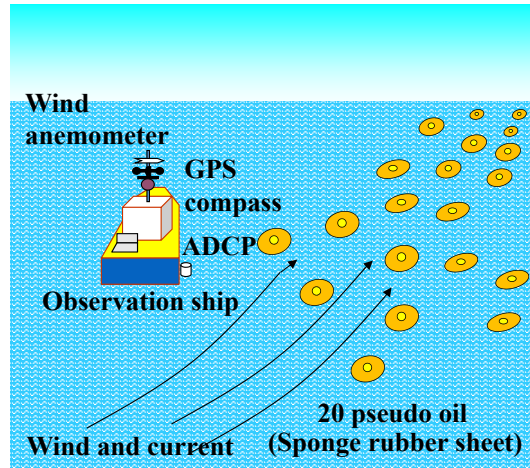


Figure 2: Experimental method

seconds and the data were averaged over 10-minute intervals. The directions of the wind and sea currents were corrected for the ship’s movement using a GPS compass (Model number; V100, Hemisphere GNSS, USA). The experiments were conducted in October and November 2012, which generated nine cases with drift times varying between 0.5 and 3.6 hours.

Experimental results of drift experiments in the real sea

Based on the method of Richardson (1926), the horizontal turbulent diffusion coefficient D_H was calculated every 10 minutes using the positions of the 20 pseudo oil objects and equation (2).

$$D_H = \frac{1}{4} \frac{\partial \sigma^2}{\partial t} \tag{2}$$

where σ^2 is the unbiased variance of the pseudo oil objects and t is time. σ^2 is calculated using equation (3).

$$\sigma^2 = \frac{1}{N-1} \sum_{in=1}^N ((x_{in} - \bar{x})^2 + (y_{in} - \bar{y})^2) \tag{3}$$

where N is the total number of pseudo oil objects, in is a particular pseudo oil object and x, y are its coordinates.

First, we compared the relationship between D_H and the wind or current velocity. Figure 4 shows the relationship between wind velocity and D_H . The horizontal axis represents the wind velocity and the

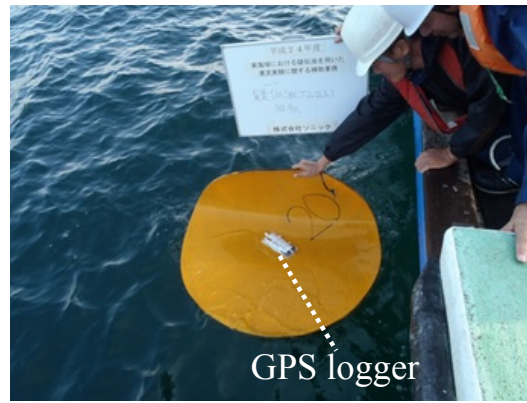


Figure 3: Pseudo oil object with GPS logger

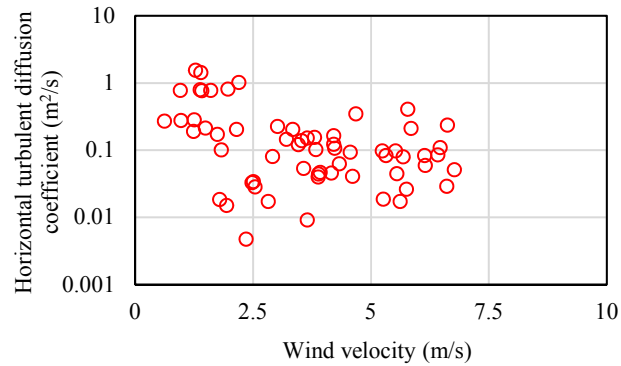


Figure 4: The relationship between wind velocity and D_H . The horizontal axis represents the wind velocity and the vertical axis the horizontal turbulent diffusion coefficient D_H .

vertical axis the horizontal turbulent diffusion coefficient D_H , which illustrates that there is no correlation between D_H and wind velocity.

Figures 5 and 6 show the relationships between current velocity and D_H and pseudo oil movement velocity and D_H , respectively, which also illustrate the absence of correlation between D_H and current velocity or pseudo oil movement velocity.

The results of Figs. 4, 5 and 6 indicated that under the weather and marine conditions experienced and the analysis methods used, a significant relationship between sea surface current velocity and D_H could not be found. Therefore, to derive an expression for the calculation of D_H , we assumed that horizontal turbulent diffusion depends on diffusion scale only.

ESTIMATION OF HORIZONTAL TURBULENT DIFFUSION COEFFICIENT FROM DRIFT EXPERIMENT RESULTS

Figure 7 illustrates the relationship between the diffusion scale L and the horizontal turbulent diffusion coefficient D_H . The horizontal axis represents the diffusion scale and the vertical axis the horizontal turbulent diffusion coefficient D_H . The diffusion scale L is defined as 3σ , based on Okubo (1971). The illustrated relationship between L and D_H appears coincident with the trend of Richardson's (1926) theory. Thus, based on this coincidence of the experimental results (64 pairs), it was assumed that the turbulent diffusion coefficient is proportional to the four-thirds power of the diffusion scale. The relationship between them is approximated by the black solid line in Fig. 7.

This regression line expresses the horizontal turbulent diffusion coefficient at the sea surface, whereas the models of Okubo (1971), Yanagi et al. (1982), and Michida et al. (2009) express horizontal turbulent diffusion coefficients under the water surface. In comparison with the other models, our regression line is larger and therefore, the horizontal turbulent diffusion coefficient at the sea surface appears greater than

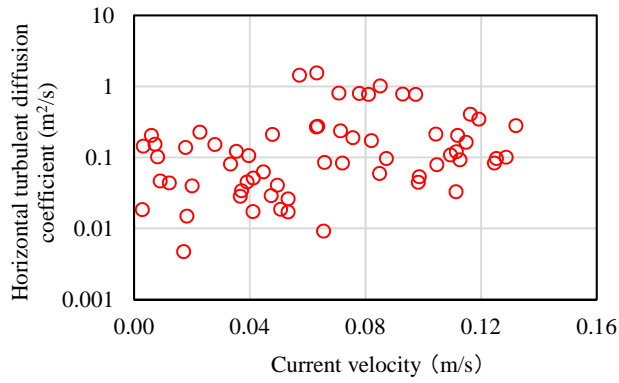


Figure 5: The relationship between current velocity and D_H . The horizontal axis represents the current velocity and the vertical axis the horizontal turbulent diffusion coefficient D_H .

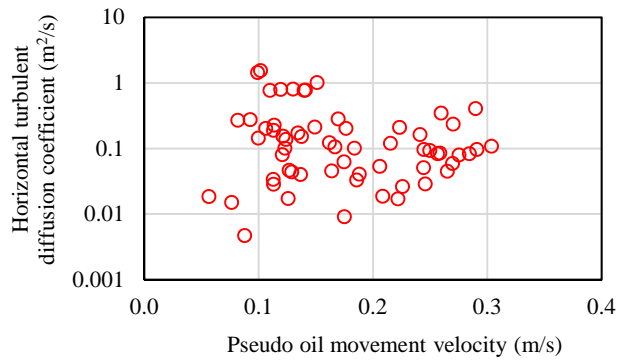


Figure 6: The relationship between pseudo oil movement velocity and D_H . The horizontal axis represents the pseudo oil movement velocity and the vertical axis the horizontal turbulent diffusion coefficient D_H .

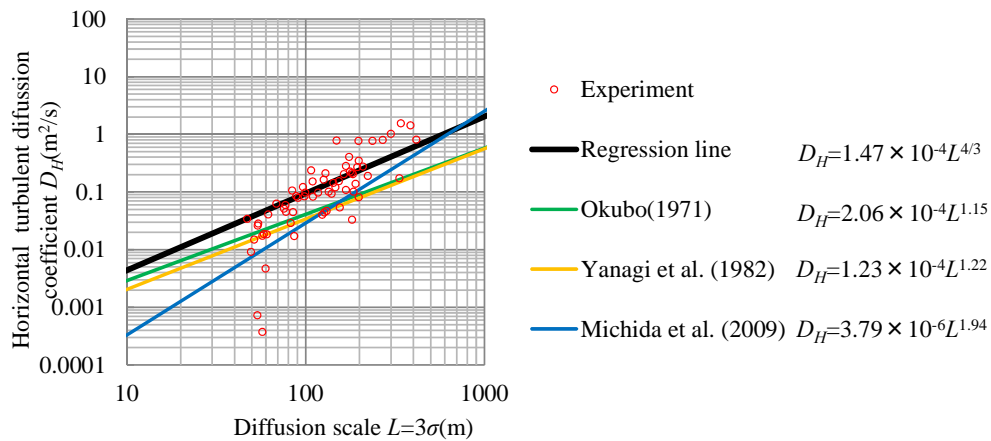


Figure 7: Relationship between diffusion scale and horizontal turbulent diffusion coefficient. Red open circles depict experimental results, black solid line represents regression line of experimental results, green line illustrates model by Okubo (1971), yellow line represents model by Yanagi et al. (1982), and blue line represents model by Michida et al. (2009).

Table 2: Calculation conditions of tidal current

Area		125° 10' 15'' E - 126° 24' 45'' E 36° 00' 15'' N - 37° 19' 45'' N
Time		2007/12/4 0:00 - 2007/12/11 11:00
Mesh number		70 × 112 × 10
Mesh size	Δx	743 m (30 s)
	Δy	925 m (30 s)
	Δz	5 m (1 - 8 layer) 10 m (9, 10 layer)
Time step	Δt	10 s
Roughness coefficient	n	0.0026
Horizontal eddy kinematic viscosity coefficient	ν_H	30 m ² /s
Vertical eddy kinematic viscosity coefficient	ν_V	0.10 m ² /s

under the water surface.

Next, we discuss the input method of the numerical simulation and the adaptivity of our regression line. The calculation of oil turbulent diffusion using the random walk technique is necessary to complement the subgrid-scale turbulence. Thus, the adaptivity of the regression line we proposed is dependent on the repetition scale of the spatial direction based on the grid size of the wind and current data. Furthermore, the turbulent flow structure, where D_H is proportional to four-thirds of the diffusion scale, is limited to the "pseudo three-dimensional isotropic range" (Toba et al., 1984).

Therefore, the horizontal turbulent diffusion coefficient D_H in the numerical simulation is simulated as follows. D_H is increased until the turbulence repetition scale L_{max} is defined by the repetition scale of the spatial direction or the pseudo three-dimensional isotropic range. The value of L is not increased further if it exceeds these conditions. Thus, D_H can be calculated using equation (4).

$$D_H = \begin{cases} 1.47 \times 10^{-4} (l_i)^{4/3} & l_i < L_{max} \\ 1.47 \times 10^{-4} (L_{max})^{4/3} & l_i \geq L_{max} \end{cases} \quad (4)$$

where l_i means the distance of oil particle i to the center of all oil particles. The maximum value of the pseudo three-dimensional isotropic range is 1.0×10^4 m (Toba et al., 1984); thus, turbulence repetition scale L_{max} is set to 1.0×10^4 m as a maximum, and to smaller values depending on the repetition scale of the spatial direction.

HINDCAST SIMULATION USING DERIVED HORIZONTAL TURBULENT DIFFUSION MODEL

A hindcast simulation was conducted using the simulation model of oil transport on a water surface of the Port and Airport Research Institute (PARI) (Matsuzaki and Fujita, 2014) to validate the efficacy of the derived diffusion model (equation(4)). The object of the hindcast simulation was the oil spill incident involving the tanker Hebei Spirit, off the Taean Coast in the Republic of Korea.

The calculation considerations were as follows. The ocean currents are not strong in the Yellow Sea, and there are no large river inflows. Therefore, the advection force was calculated based on tidal and wind currents only. The tidal current was calculated using the Storm surge and Tsunami simulator in Oceans and Coastal areas Multi-Level (STOC-ML) model (Tomita and Kakinuma, 2005). Table 2 presents the conditions used to calculate the tidal current. Tide level was set at the open boundary using a tide-level estimation model (Matsumoto et al., 2000). The bathymetry was obtained from the General Bathymetric Chart of the Oceans (GEBCO) 30-second-mesh data.

Wind current was simulated using the wind coefficient method, as follows.

$$U_{wi} = C_w W_{10i} \quad (5)$$

where U_{wi} is the velocity of movement of oil particle i , C_w is the wind coefficient, W_{10i} is wind velocity above the sea surface at the location of oil particle i , and C_w was set to 0.03 (Matsuzaki and Fujita, 2014).

Table 3: Calculation conditions for the oil transport simulation model

Oil spill site	126° 03.01' E, 36° 52.01' N
Particle number	1,200
Volume of particle	10 m ³ /particle
Time step	10 s
Oil spill time and oil spill flow rate	12/7 8:00 - 12/9 0:00 211 m ³ /hour 12/9 0:00 - 12/11 11:00 61 m ³ /hour

Table 4: Comparison between observation and simulation results of the oil spill area

Time		12/7 18:00	12/8 18:00	12/11 10:40
Oil spill area (km ²)	A:Observation area	31	110	1,195
	B:Simulation area	30	110	1,168
Area ratio of observation to simulation	A/B	1.04	1.00	1.02

The wind data used had a grid size of 10 km and were obtained from the Grid Point Value Meso-Scale Model (GPV MSM) reanalysis data from the Japan Meteorological Agency.

Table 3 displays the calculation conditions used in the model of oil transport simulation. Two cases were used for the diffusion coefficient. One was the method we proposed, where the turbulence repetition scale L_{max} was set to 1.0×10^4 m based on the repetition scale of the spatial direction of the wind data. The other method used a constant value ($D_H = 1, 10, 100$ m²/s).

Figure 8 illustrates the good agreement between the observed and simulated results of the oil spill area.

Table 4 presents a comparison of the details of the oil spill area between the observed and simulated results. The observed area of the oil spill was calculated using pixel numbers from image data; the oil slick was assumed to exist uniformly within the boundary of the area (i.e., oil distribution was not considered). The simulated oil spill area was calculated as follows. The mesh to count the oil particles was set to the area of oil transport simulation, and it was assumed that oil particles existing within the mesh were distributed uniformly. The figures presented in Table 4 indicate that simulated results using the derived diffusion model agree well with the observations.

DISCUSSION

The derived diffusion model has two distinct advantages. The first is the convenience it offers users. Figure 9 shows the differences in the ratio of oil slick area between the simulation using the derived diffusion model and those using a constant value for the horizontal turbulent diffusion coefficient D_H . There is no difference between the results simulated with the derived diffusion model and those obtained using a value of $D_H = 22$ m²/s, and their simulations agree well with the observed oil slick areas. However, the simulated results using a value of $D_H = 1$ m²/s or 100 m²/s are not in good agreement. Therefore, if the best value for D_H can be selected, the simulation results will agree well with real oil diffusion. However, it is difficult for novice users to set the diffusion coefficients appropriately for onsite turbulence or calculation conditions. The derived oil diffusion model calculates the appropriate horizontal turbulent diffusion coefficient D_H automatically as part of the numerical simulation and therefore, novice users will be able to simulate real sea oil diffusion.

The second advantage is the simplicity of the model. The derived diffusion model is easy to program in other existing Lagrangian-type simulation models.

CONCLUSIONS

In this study, field measurements of oil turbulent diffusion using pseudo oil on a water surface were conducted at the mouth of Tokyo Bay in Yokosuka, Japan, during October and November 2012. Relation-

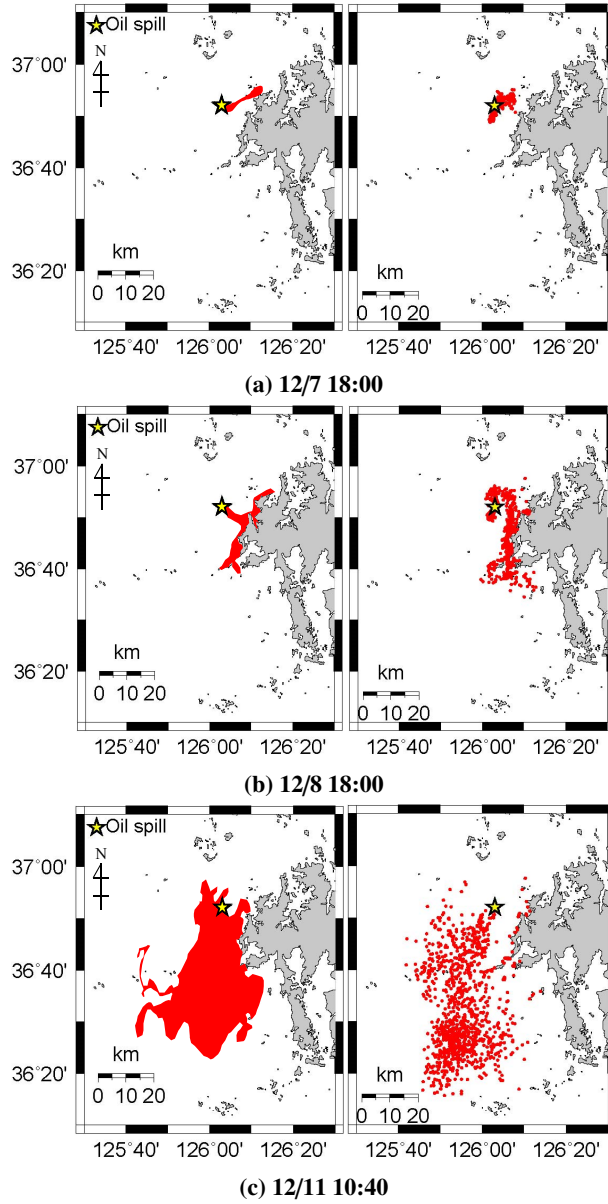


Figure 8: Illustrative comparison between observed (left-hand images) and simulated (right-hand images) results of the oil spill area

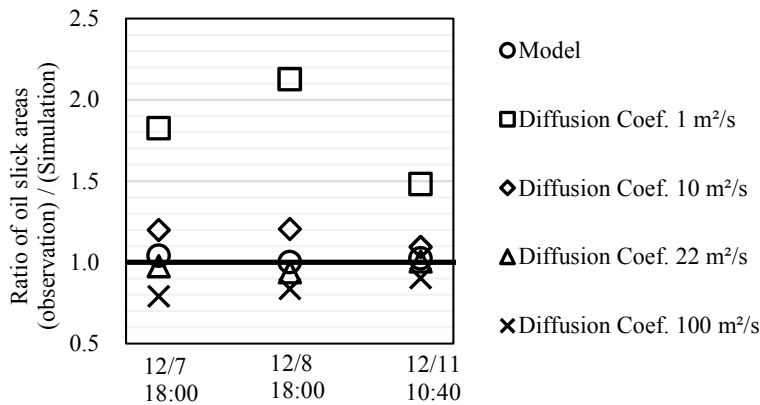


Figure 9: Differences in ratio of oil slick area between simulations using the derived diffusion model and those with a constant value for the horizontal turbulent diffusion coefficient D_H .

ships between wind and current velocity and the horizontal turbulent diffusion coefficient D_H could not be found under the weather and marine conditions and analysis methods, and the horizontal turbulent diffusion coefficient at the water surface was found to be larger than that determined by other models under the water surface.

An oil diffusion model was developed based on experimental results and a hindcast simulation, conducted using the PARI model of oil transport on a water surface, used to validate the efficacy of the derived oil diffusion model. The derived oil diffusion model calculates the appropriate horizontal turbulent diffusion coefficient D_H automatically as part of the numerical simulation. Therefore, simulations of real sea oil diffusion can be obtained by novice users. Furthermore, the derived oil diffusion model is simple and easily programmed as part of other existing Lagrangian-type simulation models.

ACKNOWLEDGEMENTS

We extend thanks to Dr. Kumagai of the National Institute for Land and Infrastructure Management for support with the wind channel tank experiments, and to Mr. Takashima of the Sonic Corporation for support with our field measurements.

REFERENCES

- ASCE Task Committee on Modeling of Oil Spills of the Water Resources Engineering Division. 1996. State-of-the-art review of modeling transport and fate of oil spills, *Journal of Hydraulic Engineering*, 122, 594-609.
- Matsumoto, K., T. Takanezawa, and M. Ooe. 2000. Ocean tide models developed by assimilating TOPEX/POSEIDON altimeter data into hydrodynamical model: a global model and a regional model around Japan, *Journal of Oceanography*, 56, 567-581.
- Matsuzaki, Y., and I. Fujita. 2014. A numerical simulation method of oil transport at sea surface and hind-cast simulation of oil spill incidents, *Journal of Japan Society of Civil Engineering*, B2, 70, 15-30. (in Japanese)
- Michida, Y., K. Tanaka, T. Komatsu, K. Ishigami, and M. Nakajima. 2009. Effects of divergence, convergence, and eddy diffusion upon the transport of objects drifting on the sea surface, *Bulletin on Coastal Oceanography*, 46, 2, 77-83.
- Okubo, A. 1971. Oceanic diffusion diagrams, *Deep-Sea Research*, 18, 789-802.
- Richardson, L. F. 1926, Atmospheric Diffusion Shown on a Distance-Neighbor Graph, *Proceedings of the Royal Society of London*, 110, 756, 709-737.
- Toba, Y., H. Kawamura, F. Yamashita, and K. Hanawa. 1984. Structure of horizontal turbulence in the Japan Sea, *Elsevier Oceanography Series*, 39, 317-332

Tomita, T., and T. Kakinuma. 2005. Storm surge and tsunami simulator in oceans and coastal areas, *Report of the Port and Airport Research Institute*, 44, 2, 83-98. (in Japanese)

Yanagi, T., K. Murashita, and H. Higuchi. 1982. Horizontal turbulent diffusivity in the sea, *Deep-Sea Research*, 29, 217-226.